AAPS PharmSciTech, Vol. 13, No. 4, December 2012 (© 2012)
DOI: 10.1208/s12249-012-9854-8

Research Article

Comparative Studies on Chitosan and Polylactic-*co*-glycolic Acid Incorporated Nanoparticles of Low Molecular Weight Heparin

Tianzhi Yang,[1] Divine Nyiawung,[1] Alexandra Silber,[1] Jiukuan Hao,[2] Leanne Lai,[3] and Shuhua Bai[1,4]

Received 23 April 2012; accepted 10 September 2012; published online 28 September 2012

Abstract. This study was performed to test the feasibility of chitosan and polylactic-*co*-glycolic acid (PLGA) incorporated nanoparticles as sustained-release carriers for the delivery of negatively charged low molecular weight heparin (LMWH). Fourier transform infrared (FTIR) spectrometry was used to evaluate the interactions between chitosan and LMWH. The shifts, intensity, and broadening of the characteristic peaks for the functional groups in the FTIR spectra indicated that strong interactions occur between the positively charged chitosans and the negatively charged LMWHs. Three types of LMWH nanoparticles (NP-1, NP-2, and NP-3) were prepared using chitosan with or without PLGA: NP-1 nanoparticles were formed by polyelectrolyte complexation after single mixing, NP-2 nanoparticles were prepared by polyelectrolyte complexation after single emulsion–diffusion–evaporation, and NP-3 nanoparticles were optimized by double emulsion–diffusion–evaporation. NP-3 nanoparticles of LMWH prepared by the emulsion–diffusion–evaporation method showed significant differences in particle morphology, size, zeta potential, and drug release profile compared to NP-1 nanoparticles formed by polyelectrolyte complexation. Another ionic complex of LMWH with chitosan-incorporated PLGA nanoparticles (NP-2) showed lower drug entrapment efficiency than that of NP-1 and NP-3. The drug release rate of NP-3 was slower than the release rates of NP-1 and NP-2, although particle morphology of NP-3 was similar to that of NP-2. Cell viability was not adversely affected when cells were treated with all three types of nanoparticles. The data presented in this study demonstrate that nanoparticles formulated with chitosan–PLGA could be a safe sustained-release carrier for the delivery of LMWH.

KEY WORDS: chitosan; low molecular weight heparin; nanoparticles; PLGA.

INTRODUCTION

Nanoparticles offer a potential strategy for the targeted delivery of therapeutic drugs by prolonging their half-lives through sustained release (1,2). Critical parameters influencing the properties of nanoparticles, such as drug loading and the sustained-release profile, are the characteristics of the polymer. Chitosan, a cationic polymer, has been used for biomedical applications due to its mucoadhesivity, biodegradability, and ability to enhance the penetration of large molecules across mucosal surfaces (3). In fact, chitosan-based nanoparticles have produced excellent transfection efficiencies during *in vitro* and *in vivo* models of the delivery of DNA due to the electrostatic interactions between the cationic amino groups in the chitosan and the negatively charged phosphate groups in the DNA molecule (4). Polylactic-*co*-glycolic acid (PLGA) is another biodegradable polymer used to prepare nanoparticles or microspheres that gradually release encapsulated drugs. After encapsulation in the PLGA carriers, the drug has a significantly increased half-life due to its sustained release and protection from enzyme degradation *in vivo* (5,6). However, both polymers have limitations for drug delivery: chitosan-formed nanoparticles release their drug contents too quickly due to rapid dissolution (3), and PLGA carriers have poor encapsulation efficiency for many drugs (7,8). Evaluations of PLGA toxicology in the lung have been reported (9,10), but it remains to be shown whether this material is viable for sustained pulmonary drug delivery. Most studies have assumed that due to their biodegradability in the body and approval by the FDA, these nanoparticles do not lead to side effects or toxicity. The question about a similar deleterious effect on the lung remains open. To improve the release properties and the drug loading amount, attempts have been made to modify nanocarriers by using polymer combinations (11–13). New PLGA nanoparticles have been developed by either encapsulating chitosan within particles or coating/adsorbing chitosan onto the surface of the polymer-based carriers. Such carriers have potential advantages such as drug loading efficiency improved by electrostatic interactions

[1] Department of Basic Pharmaceutical Sciences, School of Pharmacy, Husson University, 1 College Circle, Bangor, Maine 04401, USA.
[2] Division of Pharmaceutical Sciences, James L. Winkle College of Pharmacy, University of Cincinnati, 3225 Eden Avenue, Cincinnati, Ohio 45267, USA.
[3] Department of Sociobehavioral and Administrative Pharmacy, College of Pharmacy, Nova Southeastern University, 3200 South University Drive, Fort Lauderdale, Florida 33328, USA.
[4] To whom correspondence should be addressed. (e-mail: bais@husson.edu)

and the sustained release of encapsulated or absorbed therapeutic materials from the particles (14–18).

Low molecular weight heparin (LMWH) is a negatively charged oligosaccharide used in the treatment of deep vein thrombosis and pulmonary embolism (19,20). The presence of carboxylic acid and sulfate groups in the glycosaminoglycan units of LMWH renders it a highly anionic molecule; therefore, LMWH is an unlikely candidate for direct mucosal absorption. In addition, LMWH has a relatively short half-life (approximately 3 h) in serum. As a result, the use of LMWH in a clinical setting requires subcutaneous injections once or twice a day. Over the past few years, we have been developing new formulations using absorption enhancers, liposomes, and polyelectrolyte complexes for nasal and pulmonary delivery of LMWH (21–27). Although our data showed that these new formulations significantly improved the therapeutic efficacy of LMWH by prolonging the half-life and increasing the drug entrapment efficiency for pulmonary delivery in rat models of deep vein thrombosis and pulmonary embolism, their safety and/or stability problems remain significant concerns for further studies. Recently, Paliwal *et al.* investigated the potential of chitosan-based complexes to enhance the oral bioavailability of LMWH (28). Although a significant increase in the oral bioavailability of LMWH was observed, the half-life of LMWH was not prolonged in the study. Another group prepared PLGA microspheres for the sustained release of LMWH using a solid-in-oil-in-water emulsion method (29). The *in vitro* release tests showed that LMWH was released from PLGA microspheres in a sustained manner for about 14 days. However, after inhalation, PLGA microspheres could elicit more immunity problems compared with smaller particles (30).

There are no data on the use of chitosan-incorporated PLGA nanoparticles to deliver LMWH. Furthermore, it is not known whether the physicochemical properties and drug release profiles of LMWH entrapped in chitosan–PLGA nanoparticles differ from those of an LMWH–chitosan complex and other LMWH encapsulations in PLGA microspheres. Therefore, this study attempted to develop chitosan and PLGA incorporated nanoparticle-based delivery systems for LMWH. The three optimized particles were compared based on their physicochemical characteristics (including particle surface morphology, particle size and zeta potential, drug loading efficiency/capacity, and drug release profile) and cytotoxicity studies in lung epithelial cell culture systems. An optimized nanosized system with a high drug loading efficiency and long release time could be used as a carrier for the delivery of a negatively charged LMWH *via* noninvasive routes, such as oral, nasal, and pulmonary.

MATERIALS AND METHODS

LMWH (average molecular weight and anti-factor Xa activity of 4,494 Da and 61 U/mg, respectively) was purchased from Celsus Laboratories (Cincinnati, Ohio, USA). Low molecular weight chitosan (viscosity 20–300 cP), azure A, polyvinyl alcohol (PVA), PLGA, and 3-(4,5-dimethylthiazol-2-yl)-2,5-diphenyltetrazolium bromide (MTT) were obtained from Sigma-Aldrich (St. Louis, Missouri, USA). A 16HBE14o- cell line was obtained from Dr. Ahsan's laboratory at the Texas Tech University Health Sciences Center (Amarillo, Texas, USA). Modified Eagle's medium (MEM), fetal bovine serum (FBS), penicillin, streptomycin, phosphate-buffered saline (PBS), and trypsin-EDTA were obtained from the American Tissue Culture Collection (ATCC, Rockville, Maryland, USA).

Fourier Transform Infrared Spectroscopy

Attenuated total reflectance (ATR) Fourier transform infrared (FTIR) spectra were recorded on a Nicolet Nexus 470 spectrometer (Thermo Nicolet Corp, Madison, Wisconsin, USA) using the Smart Miracle ATR accessory. The samples were positioned in the center of the sample-holding device and scanned between 2,000 and 700 cm^{-1} at a resolution of 1 cm^{-1}. The infrared (IR) scans were processed using Happ–Genzel apodization and were presented as percent transmittance on a common scale. For the FTIR studies, chitosan solution (10 mg/mL in 0.1% acetic acid), LMWH solution (500 mg/mL), and chitosan–LMWH (*w*/*w*, 3:50; 6:50; and 12:50) complexes were used for the FTIR analysis.

Preparation of LMWH Nanoparticles

As shown in Fig. 1, three types of LMWH-containing nanoparticles were prepared by different methods: (1) polyelectrolyte complexation after single mixing (NP-1), (2) polyelectrolyte complexation after single emulsion–diffusion–evaporation (NP-2), and (3) double emulsion–diffusion–evaporation (NP-3). The LMWH–chitosan nanoparticles (NP-1) were prepared using self-assembly between positively charged chitosan and negatively charged LMWH by mixing aliquots of LMWH and an acetic acid solution of chitosan (31). Briefly, the chitosan solutions were prepared by dissolving chitosan powder in 0.1% acetic acid solution with filtration through a Millipore Millex 0.45 μM filter. LMWH was dissolved in deionized water (1.0 mg/mL) and was then mixed with the chitosan solution. The resulting solution was then incubated for 30 min at room temperature for complexation. The concentration of chitosan used in the formulations was 1 mg/mL, and the final concentration of LMWH was 0.5 mg/mL (30.5 U/mL).

Chitosan-incorporated PLGA nanoparticles (NP-2) of LMWH were prepared using a two-step method. Chitosan–PLGA nanoparticles were initially prepared by a previously reported technique with modifications (11,12). Briefly, 1 mL of PLGA solution (20%, *m*/*v* in ethyl acetate) was added to an aqueous mixture containing 10 mg of PVA as a stabilizer and 3 mg of chitosan in 1 mL of water. The emulsion was homogenized at 13,500 rpm for 20 min using a Power Gen 700 homogenizer (Fisher Scientific, Pittsburgh, Pennsylvania, USA). The ethyl acetate was then evaporated for 4 h using a Buchi R-114 Rotavapor (Buchi Laboratories, Postfach, Switzerland) at a pressure of 420 mbar and room temperature. The remaining suspension was centrifuged using an Avanti J-26XP centrifuge (Beckman Coulter, Brea, California, USA) at 8,000 rpm for 10 min. The blank nanoparticles were collected by resuspending the pellets in 3 mL of distilled water. Three milliliters of a 1 mg/mL LMWH solution was then added to the chitosan–PLGA nanoparticles and stirred for 30 min to allow for complexation.

The third set of LMWH nanoparticles (NP-3) was prepared using double emulsion–diffusion–evaporation methods (32). Briefly, 0.3 mL of LMWH (10 mg/mL) was first emulsified in

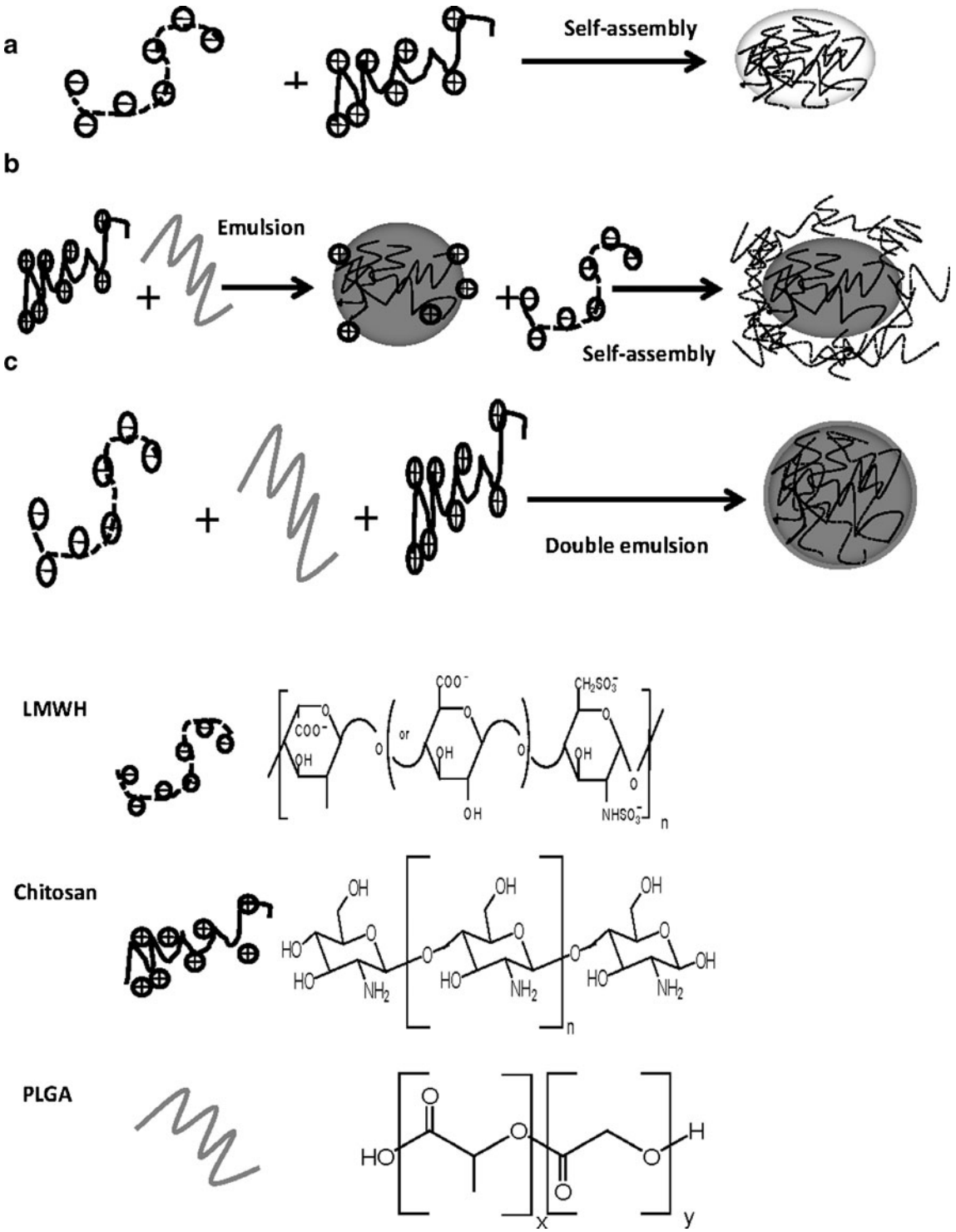

Fig. 1. Preparation scheme of LMWH complexed with chitosan, NP-1 (**a**); LMWH complexed with chitosan-incorporated PLGA nanoparticles, NP-2 (**b**); and LMWH and chitosan complex entrapped by PLGA nanoparticles, NP-3 (**c**)

1 mL of an ethyl acetate solution containing 20 mg of PLGA polymer by homogenization at 15,000 rpm for 2 min. Then, an aqueous mixture containing 10 mg of PVA and 3 mg of chitosan in 1 mL of water was added. The emulsion was homogenized at 13,500 rpm for 20 min. The ethyl acetate was then evaporated for 4 h before centrifuging at 8,000 rpm for 10 min. The final LMWH–PLGA nanoparticles were collected by resuspending the pellets in 6 mL of distilled water. All the experiments were performed in triplicate at ambient temperature.

Physicochemical Properties of LMWH Nanoparticles

The morphology of the particles was first examined using an AMRay 1820 scanning electron microscope (SEM;

AMRay Inc, Bedford, Massachusetts, USA) with a resolution of 5 nm, a magnification range of 20–150,000× and an accelerating voltage range of 100 V to 30 kV. Image capture was fully digital with an iXRF digital capture system. A drop (~50 μL) of each formulation was placed on conductive double-sided adhesive tape, air-dried, and then sputter-coated with gold under argon at an atmospheric pressure of 50 mPa.

The particle size and zeta potential of the particles were determined by using a Beckman Coulter Delsa™ Nano C nanosizing system (Beckman Corp., Brea, California, USA). Photon correlation spectroscopy was used to determine the particle size by measuring the rate of fluctuations of the laser light intensity scattered by particles as they diffused through the fluid. Electrophoretic light scattering, which determines the electrophoretic movement of charged particles under an applied electric field from the Doppler shift of the scattered light, was used to determine the zeta potential. The LMWH sample solutions (~500 μL) were dispensed into disposable measuring tubes, and the measurements were performed in triplicate. The zeta potential measurements were performed using the auto mode of at least 30 runs for each measurement.

Colorimetric Assay of LMWH

The LMWH concentrations were tested by a colorimetric assay using azure A blue dye as described in our previous studies (25,26). Briefly, 150 μL (75 μM) of azure A solution was mixed with 50 μL of LWMH standards with concentrations from 0.01 to 0.1 mg/mL and the test samples in a 96-well microplate. The resulting mixture was incubated for 30 min at room temperature. The samples were then measured by a Synergy 4 microtiter plate reader (Biotek, Winooski, Vermont, USA) at 595 nm. The concentrations of LMWH were calculated from a regression equation relating the absorbance to the LMWH concentration.

Entrapment Efficiency Measurement

The LMWH entrapment efficiency was determined by separating the nanoparticles from the dispersion medium by centrifugation as described previously (22,23). An aliquot of nanoparticles containing LMWH was mixed with 2 mL of water and was then spun at 13,500 rpm for 30 min at 15°C. The LMWH content in the supernatant was determined using the azure A colorimetric assay as described above. The entrapment efficiency was calculated as follows: $[(T - C)/T] \times 100(\%)$, where T is the initial loading amount of LMWH in the nanoparticle dispersion and C is the amount of LMWH detected in the supernatant.

Drug Release Studies

The LMWH nanoparticles (50 mg) were suspended in 10 mL of PBS buffer (pH7.4) in a flask containing 0.1% Tween 80 and incubated in a water bath at 37±1°C under gentle shaking (100 rpm) using a reciprocal shaking bath (Precision, Winchester, Virginia, USA). At various time intervals (0.2, 0.5, 1, 2, 4, 6, 8, and 24 h), 200 μL of each sample was withdrawn and centrifuged for 30 min at 16,000 rpm using a microcentrifuge (Eppendorf, Hauppauge, New York, USA). The supernatant was removed and assayed for the LMWH content with the azure A colorimetric method.

Cytotoxicity Studies

MTT is a tetrazolium salt and can form a measurable, dark blue formazan by mitochondrial dehydrogenase in living cells. The amount of blue-colored product generated from MTT is proportional to the number of living cells in the sample and is quantified by measuring the absorbance at a wavelength of 595 nm. An increase or decrease in the cell number results in an associated change in the amount of formazan formed, indicating the degree of cytotoxicity caused by the test sample (33). Human bronchial epithelial cells (16HBE14o-) were grown in MEM supplemented with 10% FBS and 100 U/mL of penicillin plus 100 U/mL of streptomycin in a humidified 37°C incubator with 5% CO_2. For the cytotoxicity studies, cell viability was measured by the MTT assay as previously described (32). Briefly, 16HBE14o- cells were seeded in flat-bottom, 96-well microtiter tissue culture plates. Immediately prior to the start of the experiment, the medium was removed from the wells, and the cells were washed with normal saline. Subsequently, the cells were incubated with 20 μL of the formulations or control samples for 4 h. The test samples contained 0.5 mg/mL of chitosan, 0.5 mg/mL of LMWH, NP-1 (0.5 mg/mL of chitosan and 0.5 mg/mL of LMWH), NP-2 (0.5 of mg/mL chitosan, 3 mg/mL of PLGA, and 0.5 mg/mL of LMWH), and NP-3 (0.5 mg/mL of chitosan, 0.5 mg/mL of LMWH, and 3 mg/mL of PLGA). Sodium dodecyl sulfate (SDS) was used at 1 mg/mL as a positive cytotoxic control. After 4 h, the treatment solutions were removed, and MTT (5 mg/mL) solution was added to each well. The cells were then incubated at 37°C for 4 h. Next, the solution in each well was removed, and acidified isopropyl alcohol (100 μL of 1% *v/v*, concentrated hydrochloric acid in isopropyl alcohol) was added. Finally, the plates were incubated at 37°C for 1 h, and the absorbance was measured on a Synergy 4 microtiter plate reader (Biotek, Winooski, Vermont, USA) at 570 nm. Each assay was performed on eight samples, and the cell viability was calculated using the following equation: $cell\,viability(\%) = \left[OD_{(sample)}/OD_{(control)}\right] \times 100$, where $OD_{(sample)}$ is the absorbance from the cells treated with the samples and $OD_{(control)}$ is from the cells treated with saline only.

DATA ANALYSIS

The data are expressed as mean±standard deviation. The LMWH entrapment efficacy, release profile, and cytotoxicity of the three types of nanoparticles were compared by analysis of variance. Differences were considered statistically significant at p values less than 0.05 on a two-tailed test.

RESULTS

FTIR Spectroscopy

Infrared spectra result from transitions between the quantized energy states of the bond or group that vibrates. Modifications specifically derived from chemical interactions and/or electrostatic interactions contribute to band shifts,

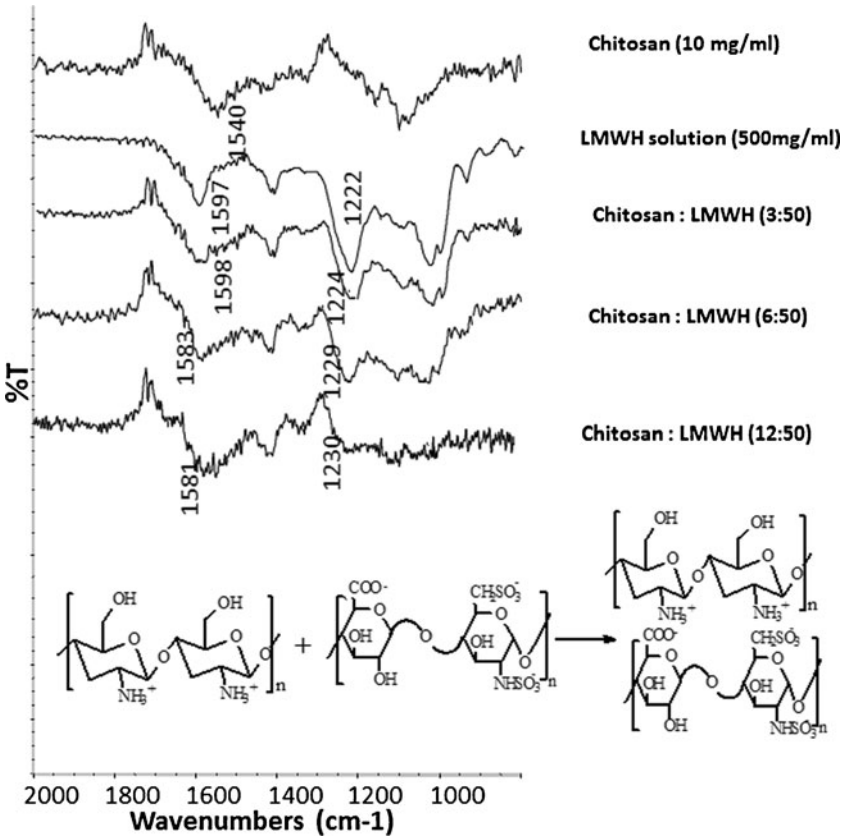

Fig. 2. FTIR spectra of chitosan, LMWH, and LMWH–chitosan complexes with increasing proportions of chitosan

changes in the peak intensity, and peak broadening in the FTIR spectra (34). The IR spectra of LMWH obtained in the aqueous solution (Fig. 2) showed peaks at 1,593 cm^{-1}, which correspond to the stretching vibrations of the C=O in the carboxylate, and at 1,222 cm^{-1}, which probably results from the S=O stretching of the sulfate ions. The peak for the stretching vibrations of the C–N groups of chitosan could be seen at 1,540 cm^{-1} (25). To investigate if the relative proportions of LWMH and chitosan present in the formulation play any role in their interaction, the IR spectra of LMWH–chitosan complexes with varying ratios (LMWH/chitosan=3:50, 6:50, and 12:50, *w*/*w*) were obtained (Fig. 2). The peak positions changed with higher concentrations of chitosan in the formulation. There were clear shifts and changes in the intensity and broadening of the peaks for the stretching vibrations of the C=O and S=O groups of the negatively charged functional groups in LMWH with the increased amounts of chitosan (Fig. 2).

Physicochemical Properties of LMWH Nanoparticles

Three types of LMWH nanoparticles were visualized by SEM. The NP-1 particles, prepared by polyelectrolyte LMWH–chitosan complexation, were significantly smaller (~300 nm) than the other two nanoparticles (~500 nm), which were formed using emulsion–diffusion–evaporation methods ($p<0.05$), although there were no significant differences between the sizes of the NP-2 and NP-3 LMWH particles (Fig. 3). Moreover, the NP-1 nanoparticles had an irregular surface shape with an ill-defined morphology. No aggregates were observed in the photomicrographs of NP-1 particles (Fig. 3a). The NP-2 and NP-3 particles appeared uniform and spherical in shape, with smooth surfaces, when the PLGA polymer was used in the preparation of the nanoparticles by the emulsion–diffusion–evaporation methods. The chitosan and PLGA-incorporated nanoparticles were evenly distributed, and few agglomerates were observed (Fig. 3b, c).

The particle size distributions of the three types of nanoparticles were further measured. The average sizes of NP-2 (635±18 nm) and NP-3 (460±126 nm) particles with LMWH were significantly greater than that of NP-1 particles (332±2 nm) ($p<0.05$), although there were no significant differences between the average particle sizes of the NP-2 and NP-3 particles (Fig. 4a). The nanometer size of the discrete average spherical particles observed using the Delsa™ Nano particle sizing system agrees with the particle sizes estimated using SEM. The data presented in Fig. 4b show zeta potentials of 25.8±0.6 mV (NP-1), −11.0±0.3 mV (NP-2), and −14.6±0.8 mV (NP-3), which were significantly different ($p<0.05$).

Entrapment Efficiency Measurement

The loading efficiency of LMWH was defined as the following percentage: the amount of LMWH loaded in chitosan or chitosan–PLGA nanoparticles divided by the total LMWH. The LMWH levels were determined by the azure A colorimetric assay. The concentration of LMWH in the supernatant was calculated from the standard calibration curve

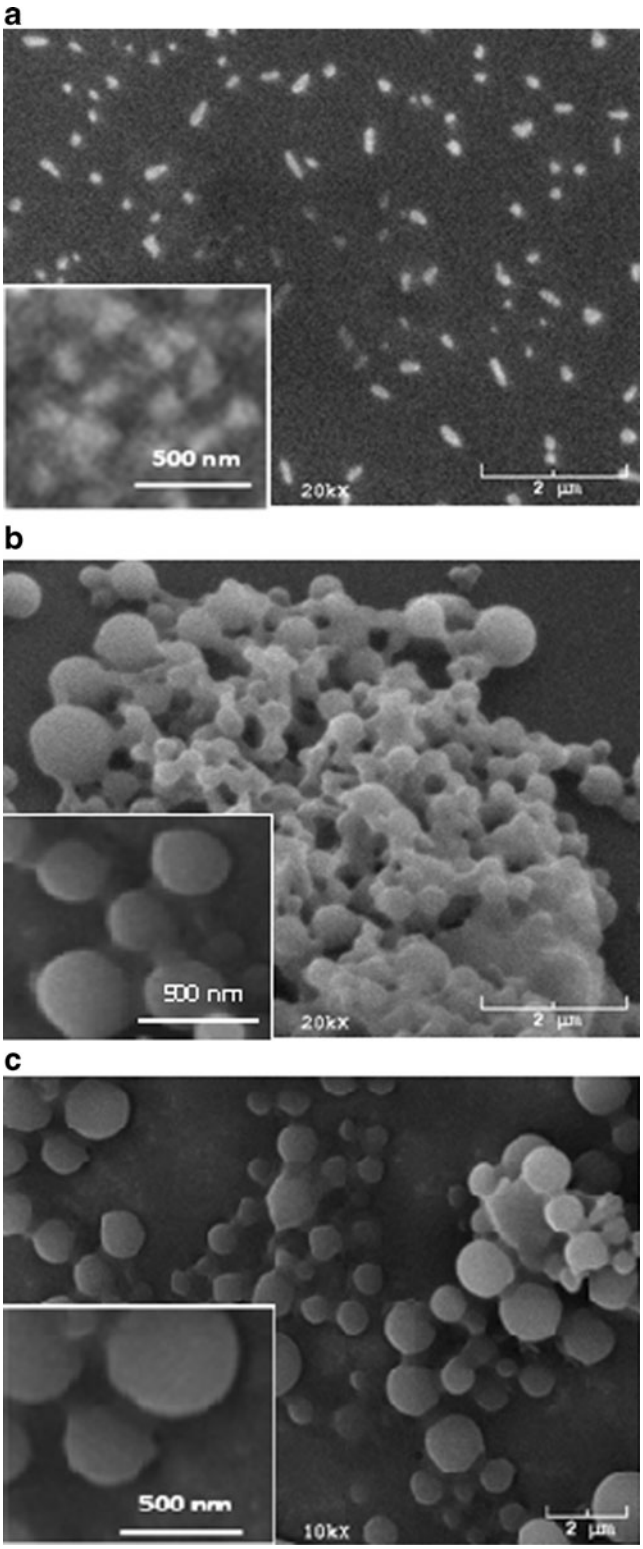

Fig. 3. SEM images of LMWH nanoparticles NP-1 (**a**), NP-2 (**b**), and NP-3 (**c**)

($y = -14.61x + 4.06, R^2 = 0.98$, where y is the absorbance and x is the LMWH concentration). A fixed amount of the drug (6 mg of LMWH) was used in the three nanoparticle formulations. When the amount of chitosan was also 6 mg, the entrapment efficiency of NP-1 particles reached 99.1±0.6%

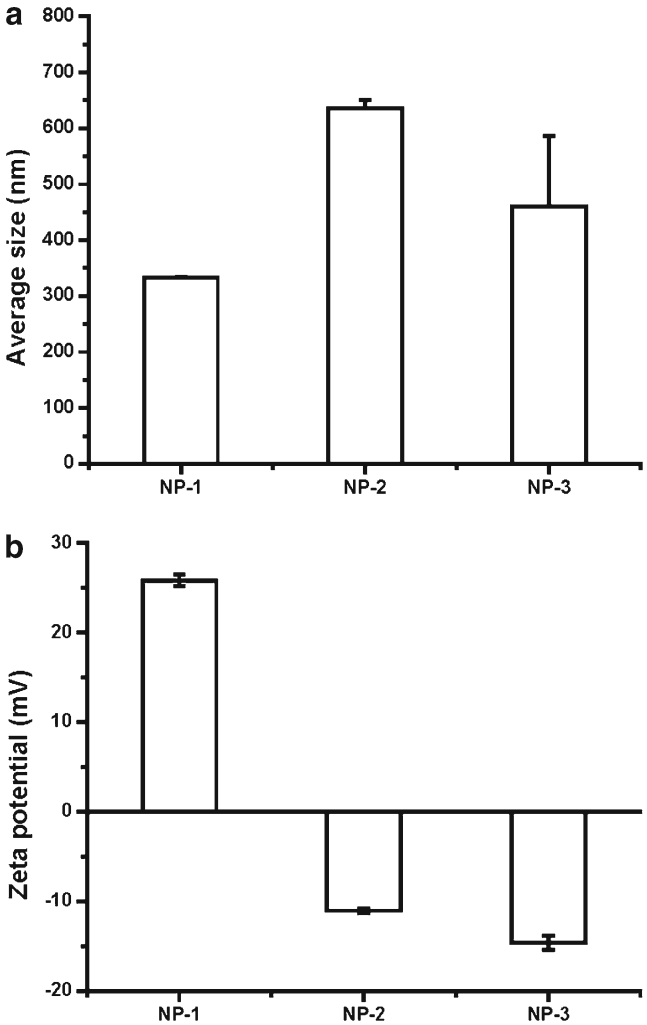

Fig. 4. Particle sizes (**a**) and zeta potentials (**b**) of LMWH nanoparticles NP-1, NP-2, and NP-3

(Fig. 5). However, when we used the same amount of LMWH and the same LMWH/chitosan ratio in the preparation of NP-2 and NP-3 particles, the entrapment efficiencies for the single

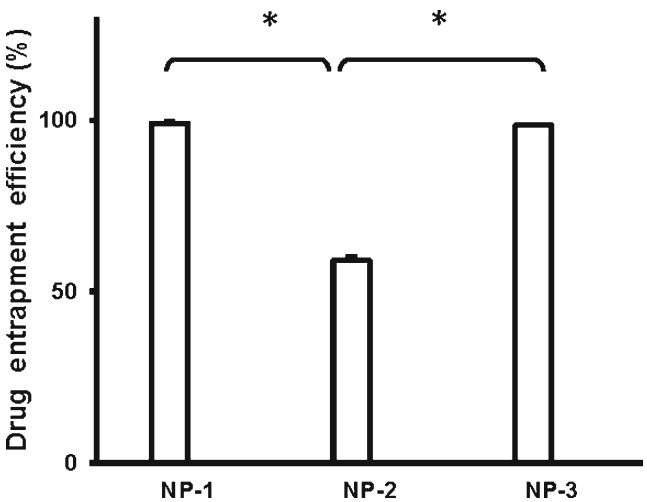

Fig. 5. Drug entrapment efficiencies of LMWH nanoparticles NP-1, NP-2, and NP-3 (* indicated significantly different, $p<0.05$)

emulsion–diffusion–evaporation and the complex method were significantly lower for the NP-2 nanoparticles (59.1±0.9%) than for the NP-3 nanoparticles prepared by the double emulsion–diffusion–evaporation method (98.5±0.4%) (Fig. 5).

In vitro Release Profiles

The amount of LMWH released from all the nanoparticle formulations was then assessed. Figure 6 shows the release profiles of LMWH from the nanoparticles prepared from a single chitosan polymer and from mixtures of chitosan with PLGA. A biphasic release pattern was observed for the NP-1 and NP-2 nanoparticles, observed as an initial burst release followed by slower first-order release kinetics. Specifically, an initial burst phase was evident in the first 0.5 h, during which large amounts of LMWH (>60%) were released rapidly. Almost complete release (>80%) was observed in the first 2 h. Although the NP-3 nanoparticles also showed a biphasic release pattern, the initial burst stage had a shorter duration. Within 0.1 h, very low amounts of LMWH (<20%) were released rapidly. The second phase of release followed slower first-order kinetics. The data showed that 50% of the LMWH was released from the PLGA NP-3 nanoparticles in a sustained manner for approximately 24 h. Therefore, the NP-3 formulation displayed a more feasible sustained-release process compared to the other nanoparticle formulations.

Cytotoxicity Studies

We used the MTT assay to examine the cytotoxic effects of LMWH nanoparticles on the 16HBE14o- cells (Fig. 7). A positive control using 1 mg/mL of SDS produced a cell viability of 47.6±5.2%. In contrast, there were high levels of viability for the 16HBE14o- cells after incubation with the chitosan-incorporated LMWH nanoparticles. All three nanoparticles had cell viabilities greater than 95% and had no significant differences compared to the control medium treatment ($p>0.05$). There were significant differences compared to the SDS-containing positive control group ($p<0.05$). Moreover, LMWH (0.5 mg/mL) alone did not reduce the viability of the 16HBE14o- cells after 4 h of exposure, although 0.5 mg/mL of chitosan in the acetic acid solution showed higher cell cytotoxicity, with a cell viability of 66.7±8.8% ($p<0.05$).

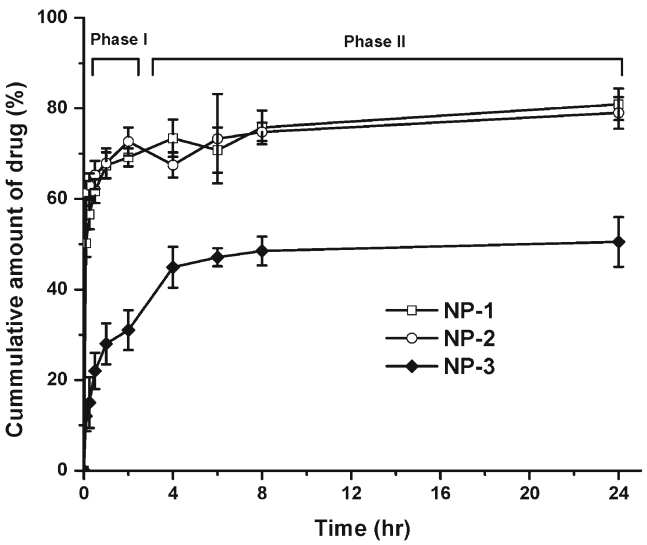

Fig. 6. Drug release profiles from chitosan or chitosan-incorporated PLGA nanoparticles NP-1, NP-2, and NP-3

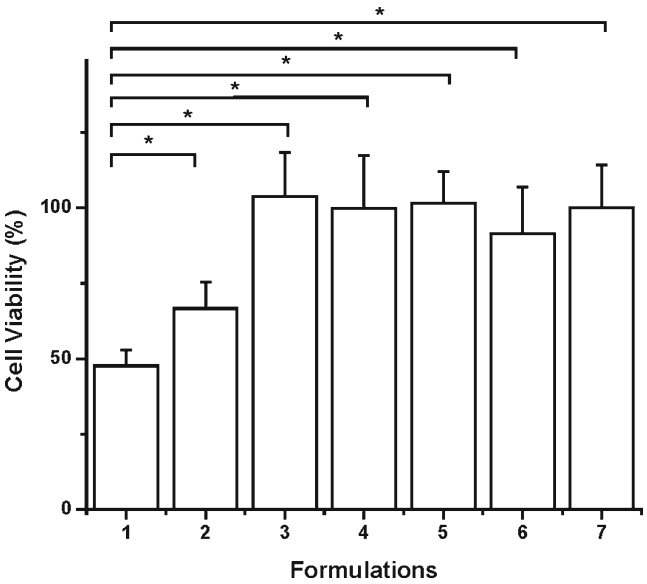

Fig. 7. Cell viabilities of 16HBE14o- cells after treatments (*1.* 1 mg/mL SDS; *2.* 0.5 mg/mL chitosan, *3.* NP-1 including 0.5 mg/mL chitosan and 0.5 mg/mL LMWH; *4.* NP-2 including 0.5 mg/mL chitosan, 3 mg/mL PLGA, and 0.5 mg/mL LMWH; *5.* NP-3 including 0.5 mg/mL chitosan, 0.5 mg/mL LMWH, and 3 mg/mL PLGA; *6.* 0.5 mg/mL LMWH; and *7.* medium control. * indicated significantly different, $p<0.05$)

DISCUSSION

FTIR spectroscopy records the specific absorption wavelength and intensity of functional groups present in a molecule. When the environment of a functional group changes, such as an interaction with an oppositely charged group or the formation of new bonds after a chemical reaction, some degree of change in its absorption bands occurs (33,34). LMWH is composed of repeating disaccharide units of D-glucosamine and uronic acid linked by 1,4 interglycosidic bonds. The main charged functional groups in the disaccharide unit of LMWH are repeating carboxylate (COO^-) and sulfate ester (SO_3^-) groups, which contribute to the highly negative charges of the LMWH molecule. The main functional groups in chitosan are the NH_2 groups or its cationic charged form, NH_3^+. In this study, there were distinct differences between the IR spectra of the LMWH–chitosan complexes and those of LMWH or chitosan alone. The positions, intensities, and the broadening of the peaks for the COO^- and SO_3^- groups of LMWH were altered. Overall, the spectra of LMWH, chitosan, and LMWH–chitosan complex suggest an electrostatic interaction between the cationic amino group of chitosan and the anionic sulfate or carboxylic acid group of LMWH (Fig. 2). Similar relationships in the FTIR spectra of LMWH and the dendrimer as well as the chitosan and chondroitin complexes were observed when the selected peak positions were plotted against the positive-to-negative charge ratios (25,35). This type of interaction could be used to form LMWH nanoparticles by polyelectrolyte complexation

through the self-assembly of positively charged chitosan and negatively charged LMWH by simple mixing, which could lead to high drug loading instead of encapsulation.

After the FTIR spectra confirmed the interaction between LMWH and chitosan, two types of nanoparticles (NP-1 and NP-2) were prepared by polyelectrolyte LMWH–chitosan complexation. Although the NP-1 nanoparticles were easier to prepare by LMWH–chitosan-charged polyelectrolyte complexation after single mixing, the morphology of the particles was varied, depending on the pH value of the chitosan solution, the chitosan concentration, the LMWH concentration, and the buffer concentration (31,36). Because the complex was formed by weak electrostatic interactions, the shapes and surfaces of the nanoparticles were not easily modified and did not appear to be well defined. The standard emulsion–solvent evaporation technique was used for formulating the PLGA nanoparticles. Various formulation factors play crucial roles in the physicochemical characteristics of the nanoparticles in biological applications (32,37). One of several factors, including homogenization speed, stabilizers (*e.g.*, PVA), the amount of the polymer, and the amount of the drug, may have a significant influence on the size distribution and morphology of the nanoparticles. In a previous study, for example, an emulsion–diffusion–evaporation technique using ethyl acetate as the organic solvent and a PVA–chitosan blend as the stabilizer yielded uniform spherical cationic nanospheres (37). In another study, when polyethyleneimine was used as the modifying agent, large porous microspheres were prepared (32). They also showed that the amount of drug was the most significant factor controlling the drug entrapment efficiency and that an increase in the amounts of the drug and the polymer resulted in a corresponding increase in the particle size (38).

We developed a simple method to optimize the modified PLGA nanoparticles. The amounts LMWH and chitosan, and their ratio, in the NP-1 nanoparticle preparations were consistent throughout the formulation screening. The PLGA amount, emulsion times, diffusion times, evaporation times, and homogenizing speed were screened to optimize the modified PLGA nanoparticles by achieving the smallest particle size (data not shown). In agreement with a previous report (37), we found that high-speed homogenization resulted in smaller globules in the emulsion and that faster dispersion of the solvent by stirring caused more irregular-sized globules in equilibrium with the continuous phase. The NP-3 nanoparticles, with an average particle size of 460 nm, uniform distribution, and smoother surface morphology, were prepared using our optimized two-step method. The NP-2 nanoparticles were prepared by eliminating one step of the complete emulsion–diffusion–evaporation method, resulting in a particle size similar to that of the NP-3 particles. An additional complexation step was incorporated after the PLGA nanoparticles were formed. After preparing LMWH nanoparticles using three different methods and observing their distinct morphologies, we further evaluated the influence of the preparation methods on the charge, LMWH encapsulation efficiency, and LMWH release profile.

Neutral or less negatively charged formulations would be expected to pass through epithelial cell layers and be absorbed into the circulation system after noninvasive delivery routes (39). Zeta potential, defined as the charge on the surface of a particulate material when the material is suspended in a solvent, is widely used to determine the surface charge of nanoparticles (40). To prepare nanoparticle formulations containing neutral charges, a fixed amount of the drug (6 mg of LMWH) was used in all three methods. The amount of chitosan in the formulation was optimized in the first simple mixing method. The NP-1 particles became positively charged upon the addition of the same amount of cationic chitosan, suggesting that the negative surface charge of the drug was neutralized by the chitosan molecules. Although we used equal amounts of LMWH and chitosan to prepare the NP-2 and NP-3 particles, they showed negative zeta potentials because another negative PLGA polymer with carboxylic acid groups was used.

The preparation methods of the nanoparticles also affected the LMWH encapsulation efficiency. During the simple mixing of LMWH and chitosan, the entrapment efficiency increased with increasing amounts of chitosan, reaching 99.1 ±0.6% for the NP-1 formulation with 6 mg of chitosan. As expected, the NP-2 PLGA nanoparticles had the lowest trapping efficiency because the positively charged chitosan was encapsulated in the nanoparticles, causing the surface of the nanoparticles to have fewer positive charges. Although this type of nanoparticle has been successfully used in the delivery of small amounts of therapeutic agents, such as DNA and small interfering RNA, the positive charges are not sufficient to neutralize the high amount of negatively charged LMWH by simple mixing of charged nanoparticles and LMWH. In contrast, a high LMWH entrapment efficiency (98.5±0.4%) was observed for the NP-3 nanoparticles produced by double emulsion–diffusion–evaporation. The chitosan molecules in the internal phase first formed complexes with LMWH. Then, the LMWH complex and the remaining free drug were encapsulated into the PLGA nanocarrier. Overall, the NP-1 and NP-3 particles displayed high entrapment efficiencies, although they were formed by different procedures.

The NP-1 and NP-2 particles showed immediate release profiles (Fig. 6). The burst phase in the release could be explained by the release process of the LMWH adsorbed on the surface of the particles with the development of a high concentration gradient across the particle surface in the NP-1 and NP-2 nanoparticles. The LMWH could be easily released from surface-associated drugs without the involvement of polymer dissolution. However, a very low drug burst release was observed for the NP-3 nanoparticles prepared with chitosan and PLGA polymers, which is probably due to the encapsulation of LMWH in the NP-3 particles. After preparation by double emulsion and diffusion processes, the LMWH in the NP-3 particles was complexed with chitosan, and then, the complex was encapsulated in the PLGA matrix. Therefore, as the PLGA gradually dissolved, the drug diffused into the external aqueous phase. This slow-release phenomenon has been reported by different research groups (41–43). One group showed that the PLGA nanoparticle release profile plateaued after 28 days, with the cumulative release remaining at approximately 41% after 40 days (42).

For core-modified nanoparticles, the amount of drug released in the initial burst phase was dependent on the

entrapment efficiency and the amount of drug associated with the surface of the particles. In addition to the entrapment efficiency, the amount of drug released was affected by the modifying agent in the carriers (32). In terms of the amount of drug released in the burst phase, the formulations can be ranked in the following order: NP-3 < NP-2 ≤ NP-1. The rate of release was dependent on the entrapment efficiency and the structure of the carrier. The combination of chitosan and PLGA in the NP-3 particles influenced the drug release profile, compared with other delivery systems. Indeed, the burst was not immediate, and the drug was continuously released slowly from the nanoparticle matrix, which resulted in lower degradation of LMWH *in vivo*. Therefore, the optimized NP-3 particles of LMWH can address the limitation of frequent administration associated with anticoagulant therapy by providing sustained release.

Lastly, we evaluated the cytotoxicity of the prepared LMWH nanoparticles. A lung epithelial cell line, 16HBE14o-, was used. The chitosan solutions were prepared by dissolving chitosan powder in 0.1% acetic acid solution, so we tested the cell viability of acetic acid. The amount of acetic acid used in the formulation did not produce significant cytotoxicity compared to the control medium ($p>0.05$, data not shown). However, chitosan in the acetic acid solution showed higher cell cytotoxicity. When chitosan was used as a polymer to prepare the LMWH-entrapped nanoparticles, a reduction in cytotoxicity was observed compared to chitosan alone. The effect of chitosan alone on cell death was likely more pronounced because of its large positive charge. The reduced cytotoxicity seen with the nanoparticles was probably because of partial neutralization or encapsulation of the positive surface charge of chitosan due to the presence of negatively charged LMWH or the coating by the PLGA polymer. In addition, the low cytotoxicity of the chitosan–PLGA LMWH nanoparticles was likely influenced by the biocompatible and biodegradable nature of the PLGA polymer and chitosan. Overall, the cytotoxicity produced by all the polymer-modified nanoparticles was comparable to that produced by blank or plain LMWH and that of the saline control. The low toxicity of the chitosan-incorporated LMWH nanoparticles could be highly desirable in future *in vivo* applications, particularly for pulmonary delivery.

CONCLUSION

Our studies show that the entrapment efficiency of LMWH in PLGA nanoparticles can be increased by incorporating chitosan. In terms of the particle morphology, the *in vitro* release behavior and cytotoxicity, the NP-3 particles, prepared by the double emulsion–diffusion–evaporation method, were optimal for sustained release. Drug release from the NP-3 particles was considerably slower than the drug release of complexes with polyelectrolytic interactions. These data demonstrated that chitosan and PLGA-based nanoparticles are a viable option for providing sustained release of LMWH to reduce dosing.

ACKNOWLEDGMENTS

We are grateful to Drs. William Lindblad and Leslie Devaud for their valuable comments and suggestions on the manuscript.

REFERENCES

1. Davis ME, Chen ZG, Shin DM. Nanoparticle therapeutics: an emerging treatment modality for cancer. Nat Rev Drug Discov. 2008;7:771–82. doi:10.1038/nrd2614.
2. Tan ML, Choong PF, Dass CR. Cancer, chitosan nanoparticles and catalytic nucleic acids. J Pharm Pharmacol. 2009;61:3–12. doi:10.1211/jpp/61.01.0002.
3. Prabaharan M, Mano JF. Chitosan-based particles as controlled drug delivery systems. Drug Deliv. 2004;12:41–57. doi:10.1080/10717540590889781.
4. Mao S, Sun W, Kissel T. Chitosan-based formulations for delivery of DNA and siRNA. Adv Drug Deliv Rev. 2010;62:12–27. doi:10.1016/j.addr.2009.08.004.
5. Astete CE, Sabliov CM. Synthesis and characterization of PLGA nanoparticles. J Biomater Sci Polym Ed. 2006;17:247–89.
6. Mundargi RC, Babu VR, Rangaswamy V, Patel P, Aminabhavi TM. Nano/micro technologies for delivering macromolecular therapeutics using poly(D,L-lactide-co-glycolide) and its derivatives. J Control Release. 2008;125:193–209. doi:10.1016/j.jconrel.2007.09.013.
7. Govender T, Stolnik S, Garnett MC, Illum L, Davis SS. PLGA nanoparticles prepared by nanoprecipitation: drug loading and release studies of a water soluble drug. J Control Release. 1999;57:171–85.
8. Barichello JM, Morishita M, Takayama K, Nagai T. Encapsulation of hydrophilic and lipophilic drugs in PLGA nanoparticles by the nanoprecipitation method. Drug Dev Ind Pharm. 1999;25:471–6. doi:10.1081/DDC-100102197.
9. Suarez S, O'Hara P, Kazantseva M, Newcomer CE, Hopfer R, McMurray DN, *et al.* Respirable PLGA microspheres containing rifampicin for the treatment of tuberculosis: screening in an infectious disease model. Pharm Res. 2001;18:1315–9.
10. Dailey LA, Jekel N, Fink L, Gessler T, Schmehl T, Wittmar M, *et al.* Investigation of the proinflammatory potential of biodegradable nanoparticle drug delivery systems in the lung. Toxicol Appl Pharmacol. 2006;215:100–8. doi:10.1016/j.taap.2006.01.016.
11. Katas H, Cevher E, Alpar HO. Preparation of polyethyleneimine incorporated poly(D,L-lactide-co-glycolide) nanoparticles by spontaneous emulsion diffusion method for small interfering RNA delivery. Int J Pharm. 2009;369:144–54. doi:10.1016/j.ijpharm.2008.10.012.
12. Taetz S, Nafee N, Beisner J, Piotrowska K, Baldes C, Murdter TE, *et al.* The influence of chitosan content in cationic chitosan/PLGA nanoparticles on the delivery efficiency of antisense 2′-O-methyl-RNA directed against telomerase in lung cancer cells. Eur J Pharm Biopharm. 2009;72:358–69. doi:10.1016/j.ejpb.2008.07.011.
13. Ungaro F, di Villa d'Emmanuele BR, Giovino C, Miro A, Sorrentino R, Quaglia F, *et al.* Insulin-loaded PLGA/cyclodextrin large porous particles with improved aerosolization properties: *in vivo* deposition and hypoglycaemic activity after delivery to rat lungs. J Control Release. 2009;135:25–34. doi:10.1016/j.jconrel.2008.12.011.
14. Amoozgar Z, Park J, Lin Q, Yeo Y. Low molecular-weight chitosan as a pH-sensitive stealth coating for tumor-specific drug delivery. Mol Pharm. 2012;9(5):1262–70. doi:10.1021/mp2005615.
15. Hou Y, Hu J, Park H, Lee M. Chitosan-based nanoparticles as a sustained protein release carrier for tissue engineering applications. J Biomed Mater Res A. 2012;100:939–47. doi:10.1002/jbm.a.34031.
16. Zhang X, Sun M, Zheng A, Cao D, Bi Y, Sun J. Preparation and characterization of insulin-loaded bioadhesive PLGA nanoparticles for oral administration. Eur J Pharm Sci. 2012;45:632–8. doi:10.1016/j.ejps.2012.01.002.
17. Nandagiri VK, Gentile P, Chiono V, Tonda-Turo C, Matsiko A, Ramtoola Z, *et al.* Incorporation of PLGA nanoparticles into porous chitosan-gelatin scaffolds: influence on the physical properties and cell behavior. J Mech Behav Biomed Mater. 2011;4:1318–27. doi:10.1016/j.jmbbm.2011.04.019.
18. Zeng P, Xu Y, Zeng C, Ren H, Peng M. Chitosan-modified poly (D,L-lactide-co-glycolide) nanospheres for plasmid DNA delivery and HBV gene-silencing. Int J Pharm. 2011;415:259–66. doi:10.1016/j.ijpharm.2011.05.053.

19. Fareed J, Jeske W, Hoppensteadt D, Clarizio R, Walenga JM. Low-molecular-weight heparins: pharmacologic profile and product differentiation. Am J Cardiol. 1998;82:3L–10L.
20. Kleinschmidt K, Charles R. Pharmacology of low molecular weight heparins. Emerg Med Clin North Am. 2001;19:1025–49.
21. Bai S, Ahsan F. Synthesis and evaluation of pegylated dendrimeric nanocarrier for pulmonary delivery of low molecular weight heparin. Pharm Res. 2009;26:539–48. doi:10.1007/s11095-008-9769-y.
22. Bai S, Ahsan F. Inhalable liposomes of low molecular weight heparin for the treatment of venous thromboembolism. J Pharm Sci. 2010;99:4554–64. doi:10.1002/jps.22160.
23. Bai S, Gupta V, Ahsan F. Cationic liposomes as carriers for aerosolized formulations of an anionic drug: safety and efficacy study. Eur J Pharm Sci. 2009;38:165–71. doi:10.1016/j.ejps.2009.07.002.
24. Bai S, Gupta V, Ahsan F. Inhalable lactose-based dry powder formulations of low molecular weight heparin. J Aerosol Med Pulm Drug Deliv. 2010;23:97–104. doi:10.1089/jamp.2009.0745.
25. Bai S, Thomas C, Ahsan F. Dendrimers as a carrier for pulmonary delivery of enoxaparin, a low-molecular weight heparin. J Pharm Sci. 2007;96:2090–106. doi:10.1002/jps.20849.
26. Yang T, Hussain A, Bai S, Khalil IA, Harashima H, Ahsan F. Positively charged polyethylenimines enhance nasal absorption of the negatively charged drug, low molecular weight heparin. J Control Release. 2006;115:289–97. doi:10.1016/j.jconrel.2006.08.015.
27. Yang T, Mustafa F, Bai S, Ahsan F. Pulmonary delivery of low molecular weight heparins. Pharm Res. 2004;21:2009–16.
28. Paliwal R, Paliwal SR, Agrawal GP, Vyas SP. Chitosan nanoconstructs for improved oral delivery of low molecular weight heparin: *in vitro* and *in vivo* evaluation. Int J Pharm. 2012;422:179–84. doi:10.1016/j.ijpharm.2011.10.048.
29. He J, Zhou Z, Fan Y, Zhou X, Du H. Sustained release of low molecular weight heparin from PLGA microspheres prepared by a solid-in-oil-in-water emulsion method. J Microencapsul. 2011;28:763–70. doi:10.3109/02652048.2011.629740.
30. Thomas C, Gupta V, Ahsan F. Particle size influences the immune response produced by hepatitis B vaccine formulated in inhalable particles. Pharm Res. 2010;27:905–19. doi:10.1007/s11095-010-0094-x.
31. Sun W, Mao S, Mei D, Kissel T. Self-assembled polyelectrolyte nanocomplexes between chitosan derivatives and enoxaparin. Eur J Pharm Biopharm. 2008;69:417–25. doi:10.1016/j.ejpb.2008.01.016.
32. Rawat A, Majumder QH, Ahsan F. Inhalable large porous microspheres of low molecular weight heparin: *in vitro* and *in vivo* evaluation. J Control Release. 2008;128:224–32. doi:10.1016/j.jconrel.2008.03.013.
33. Mosmann T. Rapid colorimetric assay for cellular growth and survival: application to proliferation and cytotoxicity assays. J Immunol Methods. 1983;65:55–63.
34. Markovich RJ, Pidgeon C. Introduction to Fourier transform infrared spectroscopy and applications in the pharmaceutical sciences. Pharm Res. 1991;8:663–75.
35. Kaur G, Rana V, Jain S, Tiwary AK. Colon delivery of budesonide: evaluation of chitosan-chondroitin sulfate interpolymer complex. AAPS PharmSciTech. 2010;11:36–45. doi:10.1208/s12249-009-9353-8.
36. Liu Z, Jiao Y, Liu F, Zhang Z. Heparin/chitosan nanoparticle carriers prepared by polyelectrolyte complexation. J Biomed Mater Res A. 2007;83:806–12. doi:10.1002/jbm.a.31407.
37. Ravi Kumar MNV, Bakowsky U, Lehr CM. Preparation and characterization of cationic PLGA nanospheres as DNA carriers. Biomaterials. 2004;25:1771–7. doi:10.1016/j.biomaterials.2003.08.069.
38. Awotwe-Otoo D, Zidan AS, Rahman Z, Habib MJ. Evaluation of anticancer drug-loaded nanoparticle characteristics by nondestructive methodologies. AAPS PharmSciTech. 2012;13:611–22. doi:10.1208/s12249-012-9782-7.
39. Braun CS, Vetro JA, Tomalia DA, Koe GS, Koe JG, Middaugh CR. Structure/function relationships of polyamidoamine/DNA dendrimers as gene delivery vehicles. J Pharm Sci. 2005;94:423–36.
40. Wilhelm P, Stephan D. On-line tracking of the coating of nanoscaled silica with titania nanoparticles *via* zeta-potential measurements. J Colloid Interface Sci. 2006;293:88–92. doi:10.1016/j.jcis.2005.06.047.
41. Yang R, Yang SG, Shim WS, Cui F, Cheng G, Kim IW, *et al.* Lung-specific delivery of paclitaxel by chitosan-modified PLGA nanoparticles *via* transient formation of microaggregates. J Pharm Sci. 2009;98:970–84. doi:10.1002/jps.21487.
42. Wu J, Ding D, Ren G, Xu X, Yin X, Hu Y. Sustained delivery of endostatin improves the efficacy of therapy in Lewis lung cancer model. J Control Release. 2009;134:91–7. doi:10.1016/j.jconrel.2008.11.004.
43. Nair KL, Jagadeeshan S, Nair SA, Kumar GS. Biological evaluation of 5-fluorouracil nanoparticles for cancer chemotherapy and its dependence on the carrier, PLGA. Int J Nanomed. 2011;6:1685–97. doi:10.2147/IJN.S20165.